Technical University of Denmark

Design and optimisation of organic Rankine cycles for waste heat recovery in marine applications using the principles of natural selection

Larsen, Ulrik; Pierobon, Leonardo; Haglind, Fredrik; Gabrielii, Cecilia

Link back to DTU Orbit

DTU Library
Technical Information Center of Denmark

Design and optimisation of organic Rankine cycles for waste heat recovery in marine applications using the principles of natural selection

Ulrik Larsen[a,*], Leonardo Pierobon[a], Fredrik Haglind[a], Cecilia Gabrielii[b]

[a]*Department of Mechanical Engineering, Technical University of Denmark,*
Building 403, Nils Koppels Allé, 2800 Kgs. Lyngby, Denmark
[b]*Chalmers University of Technology, Maritime Operations, SE-412 96 Gothenburg, Sweden*

Abstract

Power cycles using alternative working fluids are currently receiving significant attention. Selection of working fluid among many candidates is a key topic and guidelines have been presented. A general problem is that the selection is based on numerous criteria, such as thermodynamic performance, boundary conditions, hazard levels and environmental concerns. A generally applicable methodology, based on the principles of natural selection, is presented and used to determine the optimum working fluid, boiler pressure and Rankine cycle process layout for scenarios related to marine engine heat recovery. Included in the solution domain are 109 fluids in sub- and supercritical processes, and the process is adapted to the properties of the individual fluid. The efficiency losses caused by imposing process constraints are investigated to help propose a suitable process layout. Hydrocarbon dry type fluids in recuperated processes produced the highest efficiencies, while wet and isentropic fluids were superior in non-recuperated processes. The results suggested that at design point, the requirements of process simplicity, low operating pressure and low hazard resulted in cumulative reductions in cycle efficiency. Furthermore, the results indicated that non-flammable fluids were able to produce near optimum efficiency in recuperated high pressure processes.

Keywords: Process optimization, organic Rankine cycle, Exhaust heat recovery, Large ships, Genetic algorithm

1. Introduction

There is a strong motivation in the marine sector for increasing the propulsion system energy efficiency, mainly because of increasing fuel prices and stricter upcoming regulations. Therefore technologies suitable for converting low grade heat into power are currently being studied. One of the most promising technologies is the organic Rankine cycle (ORC), which is a relatively simple power cycle with good flexibility, in terms of efficient utilization of various heat sources. The main reason is that the working fluid can be selected to suit given temperature conditions of the heat source(s) and sink(s). Selecting the optimum working fluid is a complex task and the topic has received significant attention in the scientific literature. Recently, Wang et al. [1] presented a method for selection among 13 fluids based on a multi-objective optimisation model. In 2012 Wang et al. [2] presented a study on fluid selection for a small scale ORC plant applied for waste heat recovery from a combustion engine.

Seemingly no single fluid can fully meet the numerous requirements for the ideal working fluid in an ORC process [3, 4]. Foremost, the fluid should be thermodynamically suitable, such as having appropriate evapora-tion and condensation properties. Heat transfer properties, such as viscosity and thermal conductivity, are also highly relevant. Among non-thermodynamic concerns are environmental measures such as Global Warming Potential (GWP), corrosiveness, chemical stability over the relevant temperature range, toxicity, flammability, explosiveness, general industrial acceptance, lubrication properties and cost. Therefore the fluid evaluation process is a matter of finding the candidate that best meets multiple requirements, weighted according to their (subjective) importance in the application.

In the literature, guidelines on fluid selection based on thermodynamic properties have been proposed. A recurring focus is the slope of the saturated vapour line in a temperature-entropy fluid property plot, which categorises the fluids as wet, isentropic or dry. In order to avoid low vapour quality in the expander, wet fluids require superheating in the process, whereas isentropic and dry fluids do not [5]. Dry fluids, however, require an internal heat exchanger (recuperator) in order to avoid wasting the inherent fluid energy at the outlet of the expander [4]. Also frequently discussed in the literature is the critical point of the fluids. The main advantage of operating at supercritical pressure is that the heat uptake is non-isothermal, thus potentially raising the average temperature during heat uptake and resulting in a higher thermal efficiency [6]. Recently Kuo et al. presented promising results con-

cerning the Figure of Merit (FOM) which is a figure able to predict the ORC plant thermal efficiency based on the ratio of the sensible and latent heat [7].

With the ongoing research within formulation of equations of state (EOS) and the successive development of available EOS software packages, the number of fluids accessible for theoretical calculations is increasing. A need thus arises for a methodology to evaluate a large number of fluids and an even larger number of mixtures of two or more fluids systematically. Drescher et al. [8] presented a method used for a screening of about 700 fluids based on the plant thermal efficiency. The results from thermodynamic screening of 30+ fluids have been presented by Saleh et al. [9] and Chen et al. [4]. Tchanche et al. [10] presented a methodology of evaluation by awarding each candidate fluid either a plus or a minus sign to signify whether or not the fluid is favoured regarding a number of criteria: pressure levels, expander volume, thermal and second law efficiencies, irreversibilities, toxicity, flammability, Ozone Depletion Potential (ODP) and GWP. Twenty fluids were evaluated in a ORC process with no super heating or recuperator. Dai et al. [11] used the genetic algorithm in a parametric study to determine the optimum fluid among ten in a subcritical ORC process. Papadopoulos et al. [12] used an unconventional multi-objective approach which aims at designing the molecule of ORC working fluids by looking at the resulting heat exchanger area, cost, toxicity, flammability, environmental and thermodynamic performances of a subcritical ORC process.

This paper presents a generally applicable methodology for determining the optimum Rankine process layout and working fluid based on given boundary conditions and requirements. The method builds on the principles of natural selection using the genetic algorithm (GA) and, com-

pared with previous work, this methodology is pioneering in the sense that it includes at the same time both the process layout and working fluid selection. The evaluation is based on a number of rules which penalise solutions in order to remove thermodynamically inconsistent results. The method determines the optimal fluid among any number of working fluids (and also mixtures of fluids though this is not included in this work), while optimising the process layout to the thermodynamic properties of the fluid. Fluids are evaluated across a chosen pressure range including supercritical states. All possible solutions are included in the solution domain, i.e. wet, isentropic and dry fluids with the enabling of superheating and recuperation when thermodynamically feasible. Also included in the evaluation are requirements for physical, fire and health hazard levels.

The method is used to propose the best fluid alternatives across a relevant temperature range (180-360°C) useful for exhaust heat recovery in large ships. Focus is then on the engine design point at 255°C and the reduction of the potentially highest work output caused by imposing various constraints on the process and fluid.

A description of the proposed methodology in details is covered in section 2. Section 3 presents the findings from using the methodology. Further analysis of the results is discussed in section 4, and the main conclusions are outlined in section 5.

2. Methodology

In this section objectives, features and details of the applied methodology are explained. As the aim is to find the optimum process layout and fluid under varying constraints, the method includes processes: a) at sub- and

supercritical pressures, b) with any degree of superheating, c) with or without internal recuperator and d) with and without preheater. The methodology can be divided into three parts: a flexible ORC process model, a set of weights to confine the solutions and a genetic algorithm to find the optimum solutions.

2.1. Process

Modelling the Rankine cycle was done with Matlab R2010b using systems of equations representing each component in the cycle while using equations of state (EOS) procedures from NIST Refprop 9.0 [13] to obtain thermodynamic states. All fluid candidates and their full chemical names can be found in the appendix. A sketch of the process is shown in Figure 1. As mentioned, the recuperator is optional depending on the fluid properties.
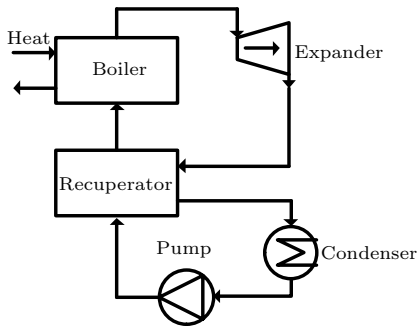

Figure 1: Sketch of the ORC process

Heat is delivered to the boiler with a heat transfer fluid called DOWthermQ, which is heated by exhaust gas from a large marine engine. This precaution is taken to avoid fire hazards in the boiler. DOWthermQ was modelled using a polynomial function which reproduces the properties of the fluid as in Ref. [14]. The working fluid is (possibly) preheated, evaporated and (possibly) superheated in the boiler at high pressure and is then injected in the expander. After the expander the hot low pressure fluid enters an internal heat exchanger (Recuperator) to heat up the cooler fluid from the pump. In the case the recuperator can heat the working fluid to reach a two-phase state, there is an elimination of the preheater heat exchanger. This is inherent in the equation systems. After the recuperator, the fluid is condensed in the condenser before entering the pump.

Table 1 lists the process conditions used. The heat source outlet temperature was defined to prevent condensation of sulphuric acid in the exhaust gas to heat transfer fluid heat exchanger. A temperature of 129°C of the heat transfer fluid is adequate to cool the exhaust gas down to 160°C. No liquid was allowed in the expander, to ensure long life and low service requirements of this component. It is stated by Chen et al. [4] that some liquid can be allowed in the expander hence investigations were also made where vapour qualities down to 85% were allowed. Allowing this

Table 1: Modelling conditions

Property	Value	Unit
Heat source outlet temperature	129	°C
Polytropic efficiency, expander	0.80	-
Isentropic efficiency, pump	0.80	-
Evaporator min. temperature difference	10	°C
Superheater approach (minimum)	20	°C
Recuperator min. temperature difference	15	°C
Condenser outlet temperature	25	°C
Minimum vapour quality, expander	1.00	-

lower limit did not however lead to higher efficiencies or other significantly changed results in general.

In order to optimise the process layout for the individual fluids, a degree of freedom for the superheater approach (ΔT_{sh}) was included. The ΔT_{sh} was defined as the difference between temperatures of the heat source at the inlet to the boiler and the working fluid at the outlet (before the expander). This enables the optimisation of the pinch points (PP) in the boiler with four possible outcomes in terms of the limiting factor in the optimisation of the cycle: A) the PP is at evaporator inlet being at the minimum allowable temperature difference, B) the minimum allowable superheater approach is reached, C) the recuperator minimum temperature difference is met, or D) none of the above in which case it is the minimum expander vapour quality which limits further optimisation.

By investigating the net work output of the process versus the pinch point temperature difference (ΔT_{pp}), it was found that the optimum work output was not synonymous with having the lowest allowable ΔT_{pp}. Thus an optimisation of the ΔT_{pp} for each individual case was justified to find the true optimum in the large solution domain.

2.2. Governing equations

In this subsection are described the main equation systems of the methodology. The expander was modelled using the assumed *polytropic* efficiency, expander inlet enthalpy (h_i) and pressure at inlet (P_i) and outlet (P_o). Due to the very wide range of expander pressure ratios investigated using the optimisation algorithm, it was chosen to use a polytropic efficiency in order to have a comparable level of cost and technology of the expander. The outlet enthalpy was found by dividing the expander into an adequate number of stages (500) such that the resulting *isentropic* efficiency was independent of the number of stages.

In order to make sure that solutions were limited to ones with acceptable vapour quality in the expander, the quality (x) was tested at all stages in the expander using EOS calls $x = x(h, p)$. The pump was modelled using an assumed isentropic efficiency. A polytropic efficiency would be preferred, but to reduce computational time and since this margin is of minor influence on the cycle efficiency, this simplification was accepted.

In the recuperator there are two temperature differences which may limit the heat transfer from the stream

entering from the expander to the cold stream entering from the pump: firstly, the internal difference (ΔT_{int}) between the entering cold stream ($T_{c,i}$) and the exiting hot stream ($T_{h,o}$), and secondly, the external difference (ΔT_{ext}) that allows the heat transfer fluid to be cooled down to a specific temperature thereby limiting the inlet temperature of working fluid to the boiler. The inlet conditions to the recuperator are known from the pump and expander equations, and with no pressure loss applied, the recuperator was described by:

$$T_{h,i} = T(P_{h,i}, h_{h,i}) \tag{1}$$
$$T_{c,i} = T(P_{c,i}, h_{c,i}) \tag{2}$$
$$T_{h,o} = T_{c,i} + \Delta T_{int} \tag{3}$$
$$h_{h,o} = h(P_{h,o}, T_{h,o}) \tag{4}$$
$$\Delta h_{max} = h_{h,i} - h_{h,o} \tag{5}$$
$$h_{c,o} = h_{c,i} + \Delta h_{max} \tag{6}$$
$$T_{c,o} = T(P_{c,o}, h_{c,o}) \tag{7}$$
$$\textbf{if } T_{c,o} > T_{h,i} - \Delta T_{int} \tag{8}$$
$$\textbf{then } T_{c,o} = T_{h,i} - \Delta T_{int} \tag{9}$$
$$\textbf{if } T_{c,o} > T_{h,o} - \Delta T_{ext} \tag{10}$$
$$\textbf{then } T_{c,o} = T_{h,o} - \Delta T_{ext} \tag{11}$$

where h is specific enthalpy, P is pressure, subscript i is inlet and o is outlet. Depending on the conditions, $h_{c,o}$ was updated according to the temperature $T_{c,o}$. Following this procedure, the second law of thermodynamics is not violated and recuperation will happen to the maximum possible degree.
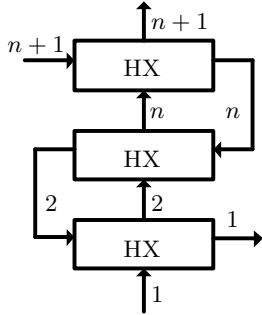

Figure 2: Sketch of heat exchangers with numbering

Modelling the boiler economiser, evaporator and superheater was done as one heat exchanger divided into n divisions, in the presented cases $n = 30$. The number of 30 was found to be a reasonable compromise between accuracy in the determination of the pinch point temperature difference and the computational time for the optimisation. Figure 2 is a sketch of the boiler heat exchangers with numbering. The heat source enters at the upper left and exits at the lower right, while the working fluid enters at the bottom and leaves at the top. With $j = 2, 3, ..., n+1$:

$$h_{c,1} = h_{p,o} \tag{12}$$
$$T_{c,o} = T_{h,i} - \Delta T_{sh} \tag{13}$$
$$h_{c,n+1} = h(P_{c,i}, T_{c,o}) \tag{14}$$
$$h_{h,n+1} = h(P_{h,i}, T_{h,i}) \tag{15}$$
$$\Delta h_{step} = (h_{c,n+1} - h_{c,1})/n \tag{16}$$
$$h_{c,j} = h_{c,1} + (j-1)\Delta h_{step} \tag{17}$$
$$T_{c,j} = T(P_{c,i}, h_{c,j}) \tag{18}$$
$$h_{h,j} = h_{h,j+1} - (\dot{m}_c/\dot{m}_h)(h_{c,j+1} - h_{c,j}) \tag{19}$$
$$T_{h,j} = T(P_{h,i}, h_{h,j}) \tag{20}$$
$$T_{h,1} = T(P_{h,i}, h_{h,1}) \tag{21}$$
$$T_{c,1} = T(P_{c,i}, h_{c,1}) \tag{22}$$
$$\Delta T_j = T_{h,j} - T_{c,j} \tag{23}$$
$$\Delta T_{min} = fMin(\Delta T_j) \tag{24}$$
$$\dot{m}_c(h_{c,n+1} - h_{c,1}) - \dot{m}_h(h_{h,n+1} - h_{h,1}) = 0 \tag{25}$$

where *fMin* is a Matlab function that finds the minimum value in an array of values. Subscript c is cold stream, h is hot stream, and min is minimum. Subscript p is the stream from the pump. To find the optimum superheater approach, a Matlab *fminbnd* optimisation algorithm was applied, using the *Golden section search* and *Parabolic interpolation* methods [15].

This approach is essential for the methodology because it accommodates all types of process scenarios. In subcritical cases the ΔT_{pp} between the hot and cold sides will be at the start of evaporation. In supercritical cases and when using mixtures, the location of the pinch point cannot be as easily predicted (to the authors' knowledge). Additionally, the approach does not distinguish between cases with or without preheater and with or without superheater, which provides the freedom to test processes and fluids without committing to a specific scenario.

As the approach presented here aims at providing a generic approach not dependent on the physical design of the heat exchangers, the optimisation was simplified by assuming zero pressure losses in the cycles.

2.3. Objective weights

Potentially weights may be defined for the optimisation process to provide a weighted compromise solution enabling multiple objectives. Alternatively, a Pareto front may be the desired result of an optimisation using two objectives. In the present work, weights were applied simply to discard inconsistent or unwanted solutions. The following weights were implemented:

- The physical, health and fire hazard levels of the fluid must meet requirements of the process design.

- The expander vapour quality was checked to be above a specified minimum.

4

Parameter	Setting
Generations	15
Sub-populations	15
Individuals	Pre-scan
Cross-over rate	1
Generation gap	0.8
Mutation rate	0.5
Insertion rate	0.9
Migration rate	0.2
Generations between migration	2

- Supercritical solutions are optional and so is the internal recuperator.

The effects on thermal efficiency of imposing requirements on health, fire and physical hazards were studied by using the HMIS (Hazardous Materials Identification System) framework [16]. At hazard level four the fluid is life threatening in case of exposure(s); it may ignite spontaneously with air and is able to chemically react in an explosive manner. At hazard level one the fluid may only cause irritation upon exposure; it will only burn if preheated and is chemically stable under normal conditions.

2.4. The Genetic Algorithm

Building on the principles of natural selection, the Genetic Algorithm (GA) [17] is an optimisation algorithm which optimises parameters for any given model. The parameters are emulated as genes of individuals which are part of a population. The fittest individuals are combined, as in nature, to form subsequent generations of individuals. The GA uses a stochastic approach to form the first generation of individuals. In the presented work, the *genes* were parameters (fluid and boiler pressure) to be evaluated (by the net work output) in order to obtain the inputs that result in optimal performance for the modelled system.

The number of *individuals* was set based on balancing between low computing time and high accuracy, and due to having 109 different possible working fluids, a large number of individuals was required. Table 2 lists the GA parameters used [17]. To reduce the number of individuals, a preliminary scanning was applied consisting of discarding fluids for which the condensation pressure could not be determined as well as those where the condensation pressure was higher than the maximum pressure of the cycle. Also discarded were fluid candidates which were unable to comply with the required hazard levels, as well as fluids banned or about to be banned in the near future (R115, R124, R141B, R142B, R11, R12, R21, R22, R113, R114 and R123 [4]).

3. Results

3.1. General influence of the heat source inlet temperature

Results from optimisation of the process, fluid and pressure are presented. A range of temperatures which are relevant to the heat recovery of large marine diesel engines

in general, was investigated. Figure 3 presents the three fluid candidates which result in the highest cycle efficiency, at their respective optimum processes and pressures versus the heat source inlet temperature. The boiler pressure is the optimum in the range of 5 to 120 bar, the upper limit being considered the maximum feasible for this type of application.
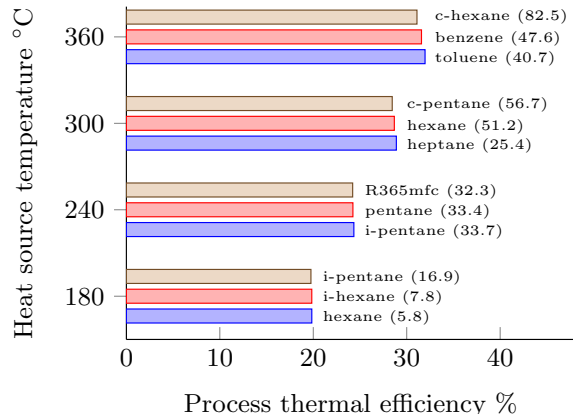

Figure 3: Optimum fluid and pressure (bar) at temperatures from 180 to 360°C with no constraints.

It is clear that the optimum pressures do not approach the upper limit of 120 bar in any of the cases. All the fluids in Figure 3 are fluids of the dry organic type, i.e. hydrocarbons with 5-7 carbon atoms and a molecular weight of 70-100 g/mol except R365mfc which contains fluor and weighs 148 g/mol.

An investigation was made of the effects on process, fluid type and pressure, and resulting efficiency caused by simplifying the cycle by removing the recuperator. In Figure 4 results show that the maximum efficiency is about 6% lower at 180°C and ranging up to 12% lower at 360°C, in comparison with recuperated cycles. Regarding the second and third best options, the decrease is higher. With the simple process layout the best fluids are not of the dry type exclusively, but instead wet (ethanol) and isentropic (acetone) while c2-butene is vaguely dry. This indicates that dry fluids are dependent on a recuperator to achieve superior efficiency. However, the difference in efficiency between the best fluid and the two other (dry) alternatives is minor (3-5%).

Several sources mention the importance of having a reduced boiler pressure. Drescher et al. [8] mention 20 bar due to safety and cost concerns. Lai et al. [18] mention that the 20 bar limit has come from legal prescriptions in certain countries. Kuo et al. [7] argue for a limit of 25 bar in order to keep material costs down (for small scale systems). The consequences of a 20 bar limit on the cycle are up to 2.5% lower efficiency for the best fluids and up to 6% for the third best fluids compared to when the limit is 120 bar; see Figure 5. The largest decreases are seen at higher source temperatures. All fluids are of the dry type,
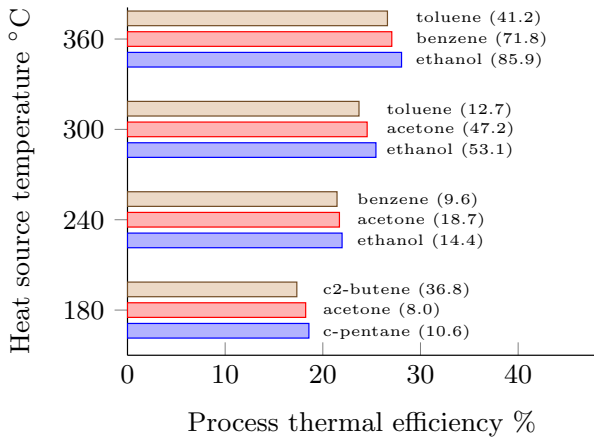
Figure 4: Optimum fluid and pressure (bar) at temperatures from 180 to 360°C with no recuperator.

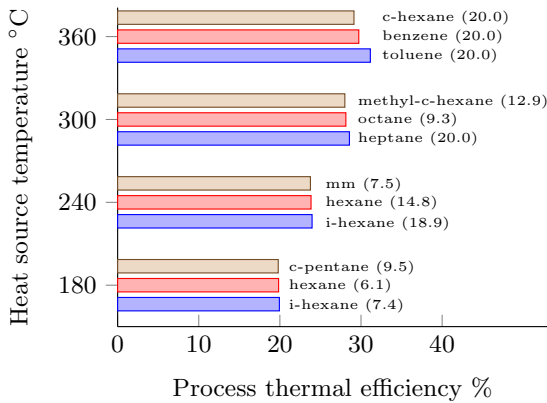and pressures are below their respective critical pressures.

Figure 5: Optimum fluid and pressure (bar) at temperatures from 180 to 360°C with limit of 20 bar on high pressure.

3.2. Engine design point

An optimisation of the process at the expected design point conditions for a MAN Diesel and Turbo low speed two-stroke diesel engine is presented in the following case. The heat source is 284°C hot exhaust gas which leaves the system at 160°C to prevent excessive corrosion in heat exchangers. The resulting heat transfer fluid temperatures are 255°C at the inlet and 129°C at the outlet of the boiler. The engine data shown in Table 3 was acquired from the MAN engine room dimensioning software [19] and the corresponding engine project guide [20].

The exhaust gas composition was found using a marine engine model derived in previous work of the authors [21], which uses a methodology derived by Rakopoulus et al. [22]. For the sake of computational efficiency, only the main species were included in the calculation of exhaust

gas enthalpy and the mass composition used was: 12.2% O_2, 72.8% N_2, 9.4% CO_2 and 5.5% H_2O.

Fluid candidates were discarded from the solution domain if one of the hazard types was at a higher level than a specified maximum. Figure 6 shows the cycle thermal efficiency for each of the hazard levels under the following constraints: NO) a high pressure limit of 120 bar with recuperator, LP) a high pressure limit of 20 bar with recuperator, SI) a simple plant layout without recuperator and a pressure limit of 120 bar and LP+SI) where the simple plant is limited to 20 bar.

Table 3: Engine parameters

Property	Value	Unit
Engine type	12K98ME-C7	-
Engine tuning method	Part load	-
Load	100	%
Cylinders	12	-
Bore	0.98	m
Stroke	2.40	m
Turbocharger type	High efficiency	-
Mean effective pressure	19.2	bar
Nominal engine speed	104	rpm
Maximum continuous rating	72240	kW
Maximum pressure	151	bar
Mean effective pressure	19.2	bar
Fuel lower heating value	42700	kJ/kg
Air flow rate	169.6	kg/s
Scavenge air pressure	4.10	bar
Scavenge air temperature	37.0	°C
Exhaust flow rate	173.1	kg/s
Fuel flow rate	3.5	kg/s
Exhaust temperature after turbocharger	284	°C
Cylinder cooling load	8570	kW

Figure 6: Effects of constraints and hazard levels
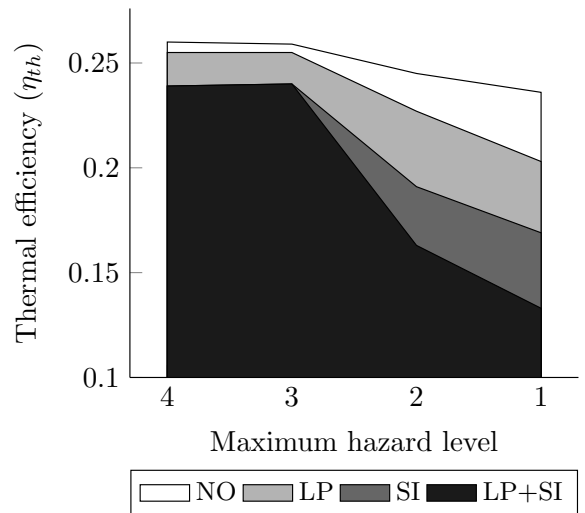
As shown in the figure, the thermal efficiencies, across constraints, are generally decreasing as the allowed hazard levels are decreasing. In general, no significant decreases are observed when moving from hazard level 4 to 3. At hazard level 2 the thermal efficiencies are markedly lower under all constraints and the same pattern is seen when moving to hazard level 1.

6

Requiring a limited maximum pressure of 20 bar is seen to cause modestly reduced efficiencies compared to the SI constraint. At levels 4 and 3, the LP constraint reduces efficiency by about 2%, while at levels 2 and 1 reductions of 7% and 14%, respectively, are seen. Under the SI constraint, the reduction is about 8% at levels 4 and 3; while at levels 2 and 1, 22% and 28% have been found, respectively. With the LP and SI constraints combined, an cumulative effect is found only at hazard levels 2 and 1, where the reductions in efficiencies are 34% and 44%, respectively.

Results of the optimisation for hazard levels up to 3 are shown in Table 4. Fluids at level 4 do not seem to be relevant, since they do not offer higher efficiencies and are extremely hazardous. The best three fluids under each of the constraints are shown in order to present alternatives with similar net work output. Again the fluid type is notably different when one compares the process with and without recuperator. The range of efficiencies among optimised processes and fluids at hazard level 3 is seen to be within about 11%.

Results from imposing hazard level 2 as the maximum are presented in Table 5. All the fluids in the table except cyclo-propane are compounds containing fluor atoms and are associated with a high global warming potential [23]. The efficiencies are strongly influenced by the constraints. It is seen that there are relatively large differences between the best fluids and the second and the third best (within the same constraints).

For cases at hazard level 1 the fluids are of the same type as for hazard level 2, with similar pressure levels, although efficiencies are lower in general.

3.3. Efficiencies across the solution domain

As argued by Kuo et al. [7] no single fluid property seems to allow the prediction of the fluid performance in the Rankine process. However, Kuo et al. found that the ratio of sensible heat transfer to latent heat of evaporation, called the Jacob number, $Ja = \bar{c}_p \Delta T / h_e$, is a good indicator of the performance of the fluid in an ORC process. $\bar{c}_p$ is the average specific heat at constant pressure, ΔT is the temperature difference during heating and h_e is the latent heat of evaporation [7]. In order to generalize the prediction ability, Kuo et al. proposed the Figure of Merit (FOM) using the condensation and evaporation temperatures (T_e): $FOM = Ja^{0.1}(T_{co}/T_e)^{0.8}$.

For the optimised results shown in Figures 3, 4 and 5, the FOM was found; see Figure 7. Excluded are results with supercritical pressures since FOM cannot be calculated in those cases.

It is seen from the figure that a linear trend can be made with very good approximation having an R^2 value (the coefficient of determination) of about 0.90. This is remarkable because the optimised cases are of very different fluids, with a relatively large range of pressures and different process configurations (with or without preheating, superheating and recuperation).
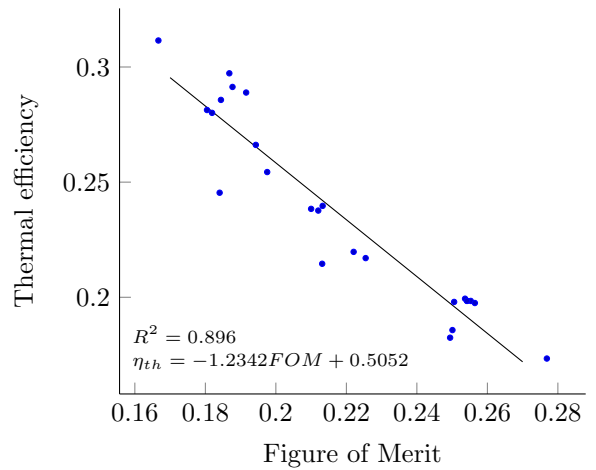
Figure 7: Thermal efficiency vs. Figure of Merit at temperatures from 180 to 360°C

The optimum thermal efficiencies across all the types of Rankine processes, fluids and pressures treated in the present work, are shown in Figure 8 along with results obtained at additional temperature levels.
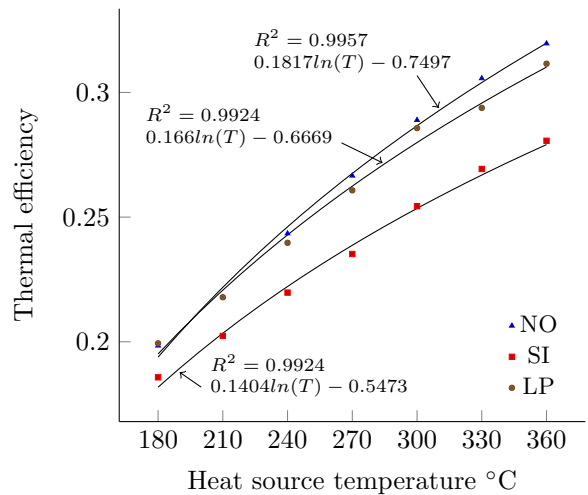
Figure 8: Thermal efficiency vs. heat source temperature

The graphs present strong correlations between the efficiencies and the temperatures for each of the treated constraints (NO, SI and LP). Thus it seems that the maximum obtainable efficiency can be predicted from the temperature alone, with the given boundary conditions.

4. Discussion

4.1. General influence of the heat source inlet temperature

In the optimisation of the individual fluid at optimum pressure and process in each of the cases shown in Figures 3, 4 and 5, the trend was that the dry fluids were optimised with the evaporator PP as the limiting factor. This

Table 4: Simulation results - hazard level 3

	Fluid (pressure in bar)	Fire hazard	Health hazard	Physical hazard	η_{th}
NO	I-hexane (29.4)	3	2	0	25.9
	Hexane (20.8)	3	2	0	25.1
	MM (9.9)	3	2	1	25.4
LP	I-hexane (20.0)	3	2	0	25.5
	Hexane (18.9)	3	2	0	25.5
	MM (9.9)	3	2	1	25.4
SI	Ethanol (19.0)	3	2	0	24.0
	Acetone (23.1)	3	2	0	23.5
	Benzene (12.0)	3	2	0	23.1
LP+SI	Ethanol (19.2)	3	2	0	24.0
	Benzene (12.0)	3	2	0	23.2
	Acetone (20.0)	3	2	0	23.2

Table 5: Simulation results - hazard level 2

	Fluid (pressure in bar)	Fire hazard	Health hazard	Physical hazard	η_{th}
NO	R245ca (37.0)	1	2	0	24.5
	R236ea (57.7)	0	1	1	23.6
	RC318 (97.2)	0	1	2	23.4
LP	R245ca (20.0)	1	2	0	22.7
	C5F12 (20.0)	2	?	?	20.8
	R236ea (19.9)	0	1	1	20.3
SI	C-Propane (99.7)	2	2	0	19.1
	R245ca (37.1)	1	2	0	18.3
	R245fa (39.6)	0	2	1	17.0
LP+SI	R245ca (20)	1	2	0	16.3
	R245fa (20)	0	2	1	14.9
	R236ea (19.9)	0	1	1	13.3

was the case in 20 of 36 cases. In 13 cases, the evaporator ΔT_{pp} was larger than the minimum allowable, and the limit for the superheater approach limited further optimisation. Those cases were mostly wet or isentropic fluids. In three cases the recuperator PP was the limiting factor, and the evaporator PP and the ΔT_{sh} were larger than the minimum allowable. Generally the evaporator ΔT_{pp} was within a few degrees of the limit for subcritical optimised cases, while the optimum efficiency was found while having up to 10 degrees larger than the minimum allowed evaporator ΔT_{pp} for some of the optimised supercritical cases.

In the ORC process with no constraints (Figure 3) the trend was that the optimum pressures were found at lower pressures when the heat source temperature was lower. The same trend was found in the constrained scenarios. At a heat source temperature of 180°C, pressures were all subcritical; while at 240°C and above, pressures were in all cases very near to the critical pressure or above. This indicates that supercritical processes are not beneficial when the heat source is cooler than about 240°C for this extensive group of fluid candidates, and conversely that supercritical processes are more efficient at this temperature and above.

This was not the case when looking at the ORC process without recuperator (Figure 4). Here, all of the cases below 360°C except one, had their optimum pressures below the critical points. Overall, the optimum pressures were slightly lower. It seems therefore that supercritical pressures do not benefit the simple ORC process when the heat source is below 360°C.

Further analysis of the large body of simulations suggests that the consequence of not allowing the pressure to exceed the critical pressure is about one percentage point lower maximum net work output in comparison.

The results seen in figures 3, 4 and 5 may represent a relatively wide range of power and thus a difference in the scale of the ORC plant. Accordingly, the typology and efficiency of the expander (in a final process design) may be different at each end of this scale. For the application and scale in the present work, a suitable expander may be a highly efficient axial turbine. Kang et al. [24] calculated isentropic efficiencies of around 80% from small scale, low temperature ORC experimental data. Colonna et al. [25] stated that a typical isentropic efficiency design value is 87%, for ORC turbines operating at the high end of the temperature range investigated in the present work. The assumed polytropic efficiency of 80% therefore seems to be reasonable for comparison within the temperature range investigated, since this value results in isentropic efficiencies of 80-82% depending on fluid and pressure ratio.

4.2. Engine design point

Regarding minimizing the hazard levels, perhaps most importantly the fire hazard in the marine application, there seems to be a clear trend in the results (Figure 6). The results suggest that there is no single fluid that can satisfy the demand for safety and high efficiency. However, the

means to obtaining both objectives seems to be to allow relatively high pressures and design the ORC process with a recuperator.

The IMO SOLAS regulations state that the flash point of a fluid in a machinery space may not be lower than 60°C. This represents a significant reduction in the number of feasible fluid candidates. Hence all the hydrocarbons can be excluded as solutions. RC318, R245fa and R236ea are all non-flammable and can as such be used. However, they have a relatively high GWP, especially RC318 with a value of 10,900 on a 100-years time horizon (CO_2-equivalent). R245fa and R236ea have GWP values of 1,020 and 1,350 respectively [26]. Domingues et al. [27] recently investigated R245fa as ORC working fluid applied to recover heat from a combustion engine. It was found that the properties of R245fa lead to high heat exchanger effectiveness and that the fluid was suitable for the application.

Other non-flammable fluids among the tested are: decafluorobutane with a GWP_{100} of 7,000, sulfur fluoride with a GWP_{100} of 23,900 (among the highest for all substances) and nitrous oxide with a relatively low GWP_{100} of 310 [23]. CO_2 is another non-flammable alternative with a low GWP. This fluid requires very high pressures to be efficient though (optimum of 18.1% efficiency at 210 bar). No other non-flammable fluids suitable for ORC were found.

Further analysis of the simulations suggested that *if* a fluid fire hazard level of 3 could be accepted, a simplified process without superheater could achieve efficiencies as high as the highest found in this study. Within this group the siloxane fluid MM is likely a good candidate with high efficiency at a low maximum pressure and low GWP. A drawback is the relatively low condensing pressure (0.06 bar at 25°C). Bombarda et al. [28] state that MM has been proposed in the literature and is in use currently as working fluid for Rankine cycles recovering heat from combustion engines. One of the leading ORC companies uses siloxanes in the same type of application [29]. This indicates that this fluid has also proven its durability and usefulness in this context.

Another fluid worth emphasizing is ethanol, which was superior within a large temperature range. Possibly mixed with water to increase the flash point (55°C) ethanol might be a good candidate as working fluid in a low pressure Rankine process with no recuperator. The maximum efficiency is nearly as good as the highest in this investigation, and the environmental profile also is good with low GWP and ODP, as well as low ecotoxicity.

4.3. Thermal stability

Toluene is already in use in the industry by a Dutch company in high temperature applications. It was selected due to its high chemical stability at elevated temperatures [30]. The stability is a key point, while information on these characteristics is only available for a few of the fluids considered in this work. Andersen et al. [31] tested the decomposition rate of normal-pentane, iso-pentane, neo-pentane, toulene and benzene under conditions relevant to high temperature ORC processes, i.e. up to 315°C and 41 bar. Benzene was found to be the most stable fluid, but decomposition was found after only a few days, though in small amounts. A 50% loss of the fluids was predicted to be in a time frame within the order of years for all of the fluids. The Andersen study highlights the need for further studies on fluid stability, as the long term consequences of using many of the ORC fluids are not described adequately. As in the present study, benzene was also found to be the best among candidates in a recent study by Vaja et al. [32] investigating a combustion engine and high temperature ORC combined cycle.

5. Conclusions

A generally applicable methodology, based on the principles of natural selection, was presented and used to determine the optimum working fluid, boiler pressure and Rankine process layout for scenarios related to marine engine heat recovery. Different solutions were obtained according to the heat source inlet temperature. The dry type organic fluids (toluene, pentanes, hexanes and heptanes) showed to be leading to the highest efficiencies in recuperated processes. In non-recuperated cycles, wet and isentropic fluids presented higher efficiencies, especially ethanol showed promising properties within the temperature range 240-360°C. Imposing a pressure limit of 20 bar on the ORC process resulted in slightly lower cycle efficiency. Supercritical pressures did result in higher efficiencies, but only with heat sources of about 300°C and hotter.

At the engine design point condition with a heat transfer fluid temperature of 255°C, the effects of pressure, process constraints and fluid hazard level were studied. Results suggested that no single fluid can be used in an ORC process satisfying the requirements of process simplicity, low pressure, high efficiency, low hazard and low environmental impact. The requirements were shown to cause accumulated reductions in the maximum achievable cycle efficiency. The high fire hazard and low flash point of the organic dry fluid type may not be accepted within the marine regulations, and only a few options remain among the studied fluids. However, R245fa and R236ea seem feasible with low hazard and near optimal efficiency at reasonable pressures, but the high GWP represents a drawback environmentally.

References

[1] Wang Z, Zhou N, Guo J, Wang X. Fluid selection and parametric optimization of organic Rankine cycle using low

temperature waste heat. Energy 2012;40(1):107–15. doi: 10.1016/j.energy.2012.02.022.

[2] Wang E, Zhang H, Fan B, Ouyang M, Zhao Y, Mu Q. Study of working fluid selection of organic Rankine cycle (ORC) for engine waste heat recovery. Energy 2011;36(5):3406–18. doi: 10.1016/j.energy.2011.03.041.

[3] Badr O, Probert S, O'Callaghan P. Selecting a working fluid for a Rankine-cycle engine. Applied Energy 1985;21(1):1–42. doi:10.1016/0306-2619(85)90072-8.

[4] Chen H, Goswami DY, Stefanakos EK. A review of thermodynamic cycles and working fluids for the conversion of low-grade heat. Renewable and Sustainable Energy Reviews 2010;14(9):3059–67. doi:10.1016/j.rser.2010.07.006.

[5] Tchanche BF, Lambrinos G, Frangoudakis A, Papadakis G. Low-grade heat conversion into power using organic Rankine cycles A review of various applications. Renewable and Sustainable Energy Reviews 2011;15(8):3963–79. doi: 10.1016/j.rser.2011.07.024.

[6] Karellas S, Schuster A. Supercritical Fluid Parameters in Organic Rankine Cycle Applications. Tech. Rep. 3; 2010. doi: 10.5541/ijot.217.

[7] Kuo CR, Hsu SW, Chang KH, Wang CC. Analysis of a 50kW organic Rankine cycle system. Energy 2011;36(10):5877–85. doi: 10.1016/j.energy.2011.08.035.

[8] Drescher U, Brüggemann D. Fluid selection for the Organic Rankine Cycle (ORC) in biomass power and heat plants. Applied Thermal Engineering 2007;27(1):223–8. doi: 10.1016/j.applthermaleng.2006.04.024.

[9] Saleh B, Koglbauer G, Wendland M, Fischer J. Working fluids for low-temperature organic Rankine cycles. Energy 2007;32(7):1210–21.

[10] Tchanche BF, Papadakis G, Lambrinos G, Frangoudakis A. Fluid selection for a low-temperature solar organic Rankine cycle. Applied Thermal Engineering 2009;29(11-12):2468–76. doi: 10.1016/j.applthermaleng.2008.12.025.

[11] Dai Y, Wang J, Gao L. Parametric optimization and comparative study of organic Rankine cycle (ORC) for low grade waste heat recovery. Energy Conversion and Management 2009;50(3):576–82. doi:10.1016/j.enconman.2008.10.018.

[12] Papadopoulos AI, Stijepovic M, Linke P. On the systematic design and selection of optimal working fluids for Organic Rankine Cycles. Applied Thermal Engineering 2010;30(6-7):760–9. doi: 10.1016/j.applthermaleng.2009.12.006.

[13] Lemmon E, Huber M, McLinden M. National Institute of Standards and Technology, Maryland, United States, Standard Reference Database 23 Reference Fluid Thermodynamic and Transport Properties-REFPROP, Software version 9.0. 2010.

[14] The Dow Chemical Company, Michigan, United States . DOWTHERM Q Heat Transfer Fluid. Tech. Rep.; 1997.

[15] Mathworks Massachusetts US. Matlab R2010b. 2010.

[16] American Coatings Association, Washington DC, United States . Hazardous Materials Identification System. 2012.

[17] Chipperfield A, Fleming PJ, Pohlheim H, Fonseca CM. Genetic Algorithm Toolbox for use with Matlab. Tech. Rep.; Department of Automatic Control and Systems Engineering, University of Sheffield, United Kingdom; Sheffield; 1994.

[18] Lai NA, Wendland M, Fischer J. Working fluids for high-temperature organic Rankine cycles. Energy 2011;36(1):199–211. doi:10.1016/j.energy.2010.10.051.

[19] Diesel & Turbo M, Copenhagen , Denmark . CEAS-ERD: Engine Room Dimensioning Software. 2013. URL www.mandieselturbo.com/ceas/index.html.

[20] Diesel & Turbo M, Copenhagen , Denmark . K98MEC7 Engine project guide. 2013. URL www.mandieselturbo.com.

[21] Scappin F, Stefansson SH, Haglind F, Andreasen A, Larsen U. Validation of a zero-dimensional model for prediction of nox and engine performance for electronically controlled marine two-stroke diesel engines. Applied Thermal Engineering 2012;37(0):344 –52. doi:10.1016/j.applthermaleng.2011.11.047.

[22] Rakopoulos C, Hountalas D, Tzanos E, Taklis G. A fast algorithm for calculating the composition of diesel combustion prod-

ucts using 11 species chemical equilibrium scheme. Advances in Engineering Software 1994;19(2):109 –19. doi:10.1016/0965-9978(94)90064-7.

[23] United States Environmental Protection Agency, Washington United States . United States Environmental Protection Agency. 2012.

[24] Kang SH. Design and experimental study of orc (organic rankine cycle) and radial turbine using r245fa working fluid. Energy 2012;41(1):514 –24. doi:10.1016/j.energy.2012.02.035. 23rd International Conference on Efficiency, Cost, Optimization, Simulation and Environmental Impact of Energy Systems, ECOS 2010.

[25] Colonna P, Harinck J, Rebay S, Guardone A. Real-Gas Effects in Organic Rankine Cycle Turbine Nozzles. Journal of Propulsion and Power 2008;24:282–94. doi:10.2514/1.29718.

[26] Montzka SA, Fraser PJ. Controlled substances and other source gases, Chapter 1 of the Scientific Assessment of Ozone Depletion: 2002, World Meteorological Organization Geneva, Switzerland. Tech. Rep.; 2003.

[27] Domingues A, Santos H, Costa M. Analysis of vehicle exhaust waste heat recovery potential using a rankine cycle. Energy 2013;49(0):71 – 85. doi:10.1016/j.energy.2012.11.001.

[28] Bombarda P, Invernizzi CM, Pietra C. Heat recovery from Diesel engines: A thermodynamic comparison between Kalina and ORC cycles. Applied Thermal Engineering 2010;30(2-3):212 –9.

[29] Vescovo R. Orc recovering industrial heat power generation from waste energy streams. Cogeneration and On-Site Power Production 2009;URL http://www.cospp.com.

[30] van Buijtenen JP. The Tri-O-Gen Organic Rankine Cycle. Tech. Rep.; Power Engineer March 2009, Delft University, The Netherlands; 2009.

[31] Andersen WC, Bruno TJ. Rapid Screening of Fluids for Chemical Stability in Organic Rankine Cycle Applications. Industrial & Engineering Chemistry Research 2005;44(15):5560–6. doi: 10.1021/ie050351s.

[32] Vaja I, Gambarotta A. Internal combustion engine (ice) bottoming with organic rankine cycles (orcs). Energy 2010;35(2):1084 –93. doi:10.1016/j.energy.2009.06.001. ECOS 2008 21st International Conference, on Efficiency, Cost, Optimization, Simulation and Environmental Impact of Energy Systems.

Appendix - List of available fluids in the Refprop library

Short name	Chemical name
acetone	propanone
ammonia	ammonia
argon	argon
benzene	benzene
butane	n-butane
butene	1-butene
carbon dioxide	carbon dioxide
carbon monoxide	carbon monoxide
carbonyl sulfide	carbon oxide sulfide
cis-butene	cis-2-butene
cyclohexane	cyclohexane
cyclopentane	cyclopentane
cyclopropane	cyclopropane
D4	octamethylcyclotetrasiloxane
D5	decamethylcyclopentasiloxane
D6	dodecamethylcyclohexasiloxane
decane	decane
deuterium	deuterium
dimethyl carbonate	dimethyl ester carbonic acid
dimethylether	methoxymethane
dodecane	dodecane
ethane	ethane
ethanol	ethyl alcohol
ethylene	ethene
fluorine	fluorine
heavy water	deuterium oxide
helium	helium-4
heptane	heptane
hexane	hexane
hydrogen (normal)	hydrogen (normal)
hydrogen sulfide	hydrogen sulfide
isobutane	2-methylpropane
isobutene	2-methyl-1-propene
isohexane	2-methylpentane
isopentane	2-methylbutane
krypton	krypton
md2m	decamethyltetrasiloxane
md3m	dodecamethylpentasiloxane
md4m	tetradecamethylhexasiloxane
mdm	octamethyltrisiloxane
methane	methane
methanol	methanol

Short name	Chemical name
methyl linoleate	methyl (Z,Z)-9,12-octadecadienoate
methyl linolenate	methyl (Z,Z,Z)-9,12,15-octadecatrienoate
methyl oleate	methyl cis-9-octadecenoate
methyl palmitate	methyl hexadecanoate
methyl stearate	methyl octadecanoate
methylcyclohexane	methylcyclohexane
MM	hexamethyldisiloxane
neon	neon
neopentane	2,2-dimethylpropane
nitrogen	nitrogen
nitrogen trifluoride	nitrogen trifluoride
nitrous oxide	dinitrogen monoxide
nonane	nonane
octane	octane
orthohydrogen	orthohydrogen
oxygen	oxygen
parahydrogen	parahydrogen
pentane	pentane
perfluorobutane	decafluorobutane
perfluoropentane	dodecafluoropentane
propane	propane
propylcyclohexane	n-propylcyclohexane
propylene	propene
propyne	propyne
sulfur dioxide	sulfur dioxide
sulfur hexafluoride	sulfur hexafluoride
toluene	methylbenzene
trans-butene	trans-2-butene
trifluoroiodomethane	trifluoroiodomethane
water	water
xenon	xenon
R11	trichlorofluoromethane
R12	dichlorodifluoromethane
R13	chlorotrifluoromethane
R14	tetrafluoromethane
R21	dichlorofluoromethane
R22	chlorodifluoromethane
R23	trifluoromethane
R32	difluoromethane
R41	fluoromethane
R113	1,1,2-trichloro-1,2,2-trifluoroethane
R114	1,2-dichloro-1,1,2,2-tetrafluoroethane

Short name	Chemical name
R115	chloropentafluoroethane
R116	hexafluoroethane
R123	2,2-dichloro-1,1,1-trifluoroethane
R1234yf	2,3,3,3-tetrafluoroprop-1-ene
R1234ze	trans-1,3,3,3-tetrafluoropropene
R124	1-chloro-1,2,2,2-tetrafluoroethane
R125	pentafluoroethane
R134a	1,1,1,2-tetrafluoroethane
R141b	1,1-dichloro-1-fluoroethane
R142b	1-chloro-1,1-difluoroethane
R143a	1,1,1-trifluoroethane
R152a	1,1-difluoroethane
R161	fluoroethane
R218	octafluoropropane
R227ea	1,1,1,2,3,3,3-heptafluoropropane
R236ea	1,1,1,2,3,3-hexafluoropropane
R236fa	1,1,1,3,3,3-hexafluoropropane
R245ca	1,1,2,2,3-pentafluoropropane
R245fa	1,1,1,3,3-pentafluoropropane
R365mfc	1,1,1,3,3-pentafluorobutane
RC318	octafluorocyclobutane